American Mineralogist, Volume 83, pages 726–739, 1998

The stability of tremolite: New experimental data and a thermodynamic assessment

Joseph V. Chernosky Jr.,[1,*] Robert G. Berman,[2] and David M. Jenkins[3]

[1]Department of Geological Sciences, University of Maine, Orono, Maine 04469, U.S.A.
[2]Geological Survey of Canada, 601 Booth Street, Ottawa, Ontario K1A 0E8, Canada
[3]Department of Geological Sciences, Binghamton University, Binghamton, New York 13902-6000, U.S.A.

Abstract

The equilibria:

$$\text{tremolite} + \text{forsterite} = 2\text{diopside} + 5\text{enstatite} + H_2O \quad (1)$$

$$\text{tremolite} + 3\text{calcite} + 2\text{quartz} = 5\text{diopside} + 3CO_2 + H_2O \quad (4)$$

have been reversed experimentally at $P_{fluid} = P_{H_2O} = 0.5$ kbar, 1.0 kbar, and 5.0 kbar and at $P_{fluid} = P_{H_2O} + P_{CO_2} = 5$ kbar, respectively. Starting materials consisted of natural tremolite (St. Gotthard, Switzerland) and quartz (Brazil), and synthetic calcite, forsterite, diopside, and enstatite mixed in stoichiometric proportions. Reaction direction was determined by comparing XRD patterns of reactant and product assemblages and by examining surface features of experimental products with an SEM.

Our new experimental data for Equilibrium 1 are consistent with the natural-tremolite results of Skippen and McKinstry (1985), who used St. Gotthard tremolite, whereas the new bracket for Equilibrium 4 is ≈25 °C lower than that of Slaughter et al. (1975) who also used St. Gotthard tremolite. Comparison of our results with other studies indicates that use of the St. Gotthard tremolite in place of synthetic tremolite in the starting material displaces these equilibria toward higher temperatures by about 25 and 5 °C, respectively. Tremolite stability differences reflected in these data, as well as in phase equilibrium data for nine additional equilibria involving synthetic and natural tremolite can be accounted for with a simple ideal on-site mixing model to describe tremolite compositional differences. Our analysis leads us to conclude, however, that tremolite growth in some experiments near the equilibrium boundary occurs with respect to metastable end-member pyroxenes used in starting materials, whereas pyroxene-stable half-brackets involve growth of stable pyroxene compositions. Thermodynamic properties for end-member tremolite, retrieved by mathematical programming analysis of the experimental phase equilibrium data with these assumptions, provide the most sound basis for prediction of calcic amphibole stability relationships in natural assemblages, as well as improved calibration of quantitative amphibole geothermobarometers. Our success in extracting consistent thermodynamic properties for end-member tremolite from experimental data obtained with both synthetic and natural tremolite, assuming the former to contain 10 mol% magnesiocummingtonite component (Jenkins 1987), can be taken either as support for the validity of this assumption or as an indication that chain multiplicity faults (Maresch et al. 1994) produce a similar degree of stabilization as this solid solution.

Introduction

Thermodynamic properties of the amphibole end-member, tremolite, are important to define for several reasons. First, they have served as a basis for calculating petrogenetic grids involving amphibole and for defining amphibolite facies metamorphic boundaries (e.g., Evans 1990). Second, various tremolite-bearing equilibria have been used for quantitative estimation of fluid component activities attending amphibolite-granulite facies metamorphism (e.g., Lamb and Valley 1988). Third, tremolite-bearing equilibria recently have been calibrated as geobarometers (Kohn and Spear 1989, 1990; Mader and Berman 1992; Mader et al. 1994) and geothermometers (Blundy and Holland 1990; Holland and Blundy 1994) that permit quantitative assessment of *P-T* conditions of amphibolite-granulite facies rocks.

Since it was first investigated hydrothermally over three decades ago (Boyd 1959), the calcic end-member amphibole tremolite, $Ca_2Mg_5Si_8O_{22}(OH)_2$, has been the subject of numerous experimental investigations: twenty-three experimentally determined data sets involving eleven tremolite-bearing equilibria have been published (Ta-

* E-mail: josephc@maine.maine.edu

TABLE 1. Published phase equilibrium data for equilibria involving synthetic and natural tremolite

1.	Tr + Fo = 2 Di + 5 En + H_2O
	Jenkins (1983): synthetic
	Skippen and McKinstry (1985): synthetic and St. Gotthard
	This study: St. Gotthard
2.	Tr = 2 Di + 3 En + Qz + H_2O
	Boyd (1959): synthetic
	Yin and Greenwood (1983): synthetic
	Jenkins and Clare (1990): Barrie Township, Ontario (TREM-12)
	Jenkins et al. (1991): synthetic
	Welch and Pawley (1991): unknown locality
3.	Tr = 2 Di + Tc
	Jenkins and Clare (1990): unknown locality (TREM-8)
	Jenkins et al. (1991): synthetic
4.	Tr + 3 Cc + 2 Qz = 5 Di + 3 CO_2 + H_2O
	Metz (1970): Campo Longo (2.59 wt% F)
	Slaughter et al. (1975): St. Gotthard
	Metz (1983): synthetic
	This study: St. Gotthard
5.	Tr + 11 Dol = 8 Fo + 13 Cc + 9 CO_2 + H_2O
	Metz (1967; 1976): Campo Longo (2.59 wt% F)
6.	5 Phl + 6 Cc + 24 Qz = 3 Tr + 5 Ksp + 6 CO_2 + 2 H_2O
	Hoschek (1973): synthetic
	Hewitt (1975): synthetic, Gouverneur (0.26 wt% F) and Richville (1.51 wt% F)
7.	Tr + 3 Cc = Dol + 4 Di + CO_2 + H_2O
	Slaughter et al. (1975): St. Gotthard
8.	5 Tc + 6 Cc + 4 Qz = 3 Tr + 6 CO_2 + 2 H_2O
	Slaughter et al. (1975): St. Gotthard
	Puhan and Metz (1987): synthetic
9.	5 Dol + 8 Qz + H_2O = Tr + 3 Cc + 7 CO_2
	Slaughter et al. (1975): St. Gotthard
	Eggert and Kerrick (1981): St. Gotthard
10.	3 Tr + 5 Cc = 11 Di + 2 Fo + 5 CO_2 + 3 H_2O
	Chernosky and Berman (1988): St. Gotthard
11.	2 Dol + Tc + 4 Qz = Tr + 4 CO_2
	Eggert and Kerrick (1981): St. Gotthard

Note: Cc = calcite; Di = diopside; Dol = dolomite; En = enstatite; Fo = forsterite; Ksp = potassium feldspar; Phl = phlogopite; Qz = quartz; Tc = talc; Tr = tremolite.

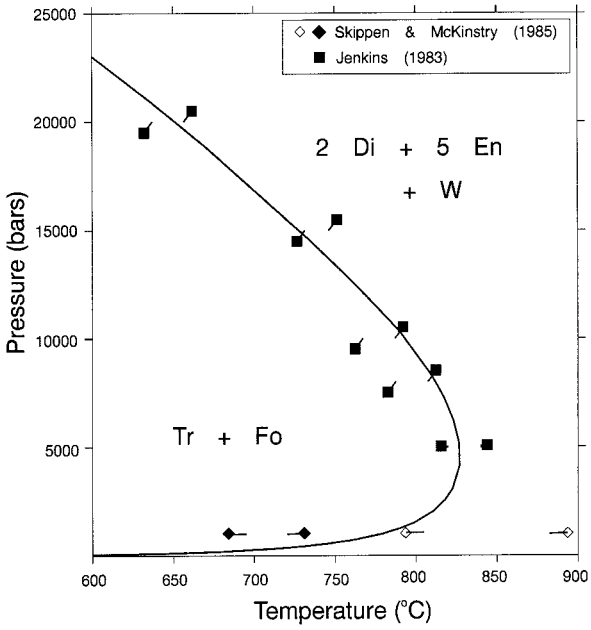

FIGURE 1. Comparison of experimental data for the equilibrium Tr + Fo = 2Di + 5En + H_2O reversed using synthetic (filled symbols) and natural (open symbols) tremolite in the starting materials. Symbols represent experimental conditions after adjustment (away from equilibrium curve) for *P-T* uncertainties, while short lines connected to symbols show nominal *P-T* conditions as well as reaction direction.

ble 1). Despite its relatively simple chemistry and widespread occurrence in metamorphic rocks, tremolite has proven to be a particularly nettlesome phase for experimentalists to work with.

Although Fe-free OH-tremolite has been synthesized from oxide mixes, glasses, and gels, a ''high quality'' synthetic product typically contains about 10% extraneous phases because of the metastable (?) persistence of clinopyroxene, with minor orthopyroxene and/or quartz and talc. Very painstaking efforts such as long-duration synthesis experiments (1800 hours) with periodic grinding (every few hundred hours) result in reported yields >95% (Troll and Gilbert 1972; Skippen 1971; Yin and Greenwood 1983; Gottschalk 1994). In addition to the presence of extraneous phases, high-resolution transmission electron microscope (HRTEM) images of synthetic tremolite (Skogby and Ferrow 1989; Ahn et al. 1991; Maresch et al. 1994) reveal the presence of chain-width defects. The nature and volume of structural defects in synthetic tremolite appear to be a function of the synthesis conditions. On the basis of the most detailed studies, it appears that stoichiometric tremolite cannot be synthesized, although a consensus has not been reached on whether the nonstoichiometry, which amounts to about 10% excess Mg, is caused by chain-multiplicity defects (Maresch et al. 1994), cummingtonite substitution (Jenkins 1987), or both.

To circumvent the problems associated with synthetic tremolite, some experimentalists have used natural tremolite in starting materials. Although very pure natural tremolite crystals occur in skarns, they invariably contain minor quantities of other elements, particularly F, small amounts of which are known to enhance significantly the stability of hydrous phases.

The entire corpus of experimental phase equilibrium data involving synthetic and several natural tremolites does not appear, on cursory inspection, to be internally consistent. For example, McKinstry and Skippen (1978) and Skippen and McKinstry (1985) reversed the equilibrium (Fig. 1).

$$\text{Tr} + \text{Fo} = 2\text{Di} + 5\text{En} + \text{H}_2\text{O} \quad (1)$$

using starting materials containing synthetic and natural (St. Gotthard) tremolite. They reported that Equilibrium 1 was displaced about 133 °C toward lower temperatures when synthetic tremolite was used in place of natural tremolite in the starting material, and they noted that this difference was larger than could be accounted for by the compositional differences between starting materials. This result suggested that synthetic tremolite might not be a suitable analogue for natural tremolite in experimental studies; the broad implication was that experimental

phase equilibrium data obtained using synthetic amphiboles may be unreliable.

Jenkins (1983) performed experiments on Equilibrium 1 at water pressures ranging from 5 to 20 kbar using synthetic tremolite and noted that the location of the univariant boundary for reaction 1, when extrapolated down to 1 kbar, was at least 50 °C higher than the reversal for synthetic tremolite reported (in abstract form) by McKinstry and Skippen (1978). Thermodynamic calculations using the database of Berman (1988) also indicate that the low-pressure experiments of Skippen and McKinstry (1985) are inconsistent with the higher-pressure data of Jenkins (1983) (Fig. 1).

Experimental work by Jenkins and Clare (1990) on the following two equilibria:

$$\mathrm{Tr} = 2\mathrm{Di} + 3\mathrm{En} + \beta\mathrm{Qz} + \mathrm{H_2O} \quad (2)$$

$$\mathrm{Tr} = 2\mathrm{Di} + \mathrm{Tc} \quad (3)$$

using both natural and synthetic tremolite showed that the use of synthetic tremolite displaced Equilibrium 2 by about 40 ± 20 °C toward lower temperatures. Jenkins and Clare (1990, p. 365) concluded that this difference could be explained by compositional variation in the tremolite and suggested that ''synthetic calcic amphiboles closely model the behavior of natural calcic amphiboles.''

Quantitative assessment of natural amphibole stability relations requires accurate thermodynamic properties for the important end-member tremolite and confidence that these properties can be applied to natural amphiboles. We have reinvestigated Equilibrium 1 as well as the equilibrium:

$$\mathrm{Tr} + 3\ \mathrm{Cc} + 2\ \mathrm{Qz} = 5\ \mathrm{Di} + 3\ \mathrm{CO_2} + \mathrm{H_2O} \quad (4)$$

at low pressures using the same natural tremolite from St. Gotthard, Switzerland, as used by Slaughter et al. (1975) and by Skippen and McKinstry (1985) to resolve some of the inconsistencies among the phase equilibrium data and thermodynamic properties for synthetic and natural tremolite. We also present a critical evaluation of a more extensive set of phase equilibrium data than considered by Jenkins and Clare (1990) consisting of eleven equilibria involving natural and synthetic tremolite. Included in this set are the new experimental data reported in this paper, recent data for Equilibrium 2 using a natural F-free tremolite (Welch and Pawley 1991), as well as the data of Metz (1983) for Equilibrium 4 with synthetic tremolite that were not used in the thermodynamic analyses of Berman (1988) or Holland and Powell (1990).

Experimental methods

Procedure

Experiments at the University of Maine were conducted in 30.5 cm long, horizontally mounted, cold-seal hydrothermal vessels machined from Haynes Alloy no. 25 (stellite) or René 41. Each vessel was connected to its own 15.2 cm Astra pressure gauge. At the initiation of an experiment, the pressure reading on the Astra gauge was referenced to one of two factory-calibrated, 40.6 cm Heise bourdon-tube gauges certified by the manufacturer as accurate to ±0.1% of full scale (0–4000 bars and 0–7000 bars). The Heise gauges were maintained at atmospheric pressure except when calibrating the Astra gauges. Minor fluctuations in pressure resulting from temperature drift did occur; however, experiments that experienced pressure changes greater than about 50 bars were discarded. Pressures are believed accurate to within ±50 bars of the stated value.

The temperature of each experiment was measured daily with a sheathed thermocouple positioned adjacent to the sample in a well drilled into the base of the pressure vessel parallel to the vessel bore. Thermocouples were calibrated at atmospheric pressure after each experiment by placing a previously calibrated ''standard'' thermocouple within the pressure vessel and noting the difference in temperature between the external and standard thermocouple. Temperature corrections were typically <5 °C. This procedure ensures internal consistency among all pressure vessels and, most importantly, allows one to monitor changes in the calibration of the external thermocouples with time. Calibrations at atmospheric pressure indicate that temperature gradients in the pressure vessels were <1 °C over a working distance of 3.0 cm. Hence, uncertainty resulting from a temperature gradient along the 1.25 cm long gold sample containers was considered negligible. We believe that the principal source of uncertainty in the temperatures stated in Tables 2 and 3 results from daily fluctuations, which are reported as ±2 standard deviations about the mean temperature.

Experiments at Binghamton University were performed in an internally heated vessel similar to that described by Holloway (1971); Ar was used as a pressure medium. Pressures were monitored continuously throughout the duration of an experiment and were measured with a precision of ±10 bars using both a bourdon-tube gauge and a factory calibrated manganin cell (Harwood Engineering).

The temperature gradient across the sample capsule was measured with two Inconel-sheathed, grounded, type K thermocouples whose tips were separated by about 9 mm and positioned to span the length of the capsule. Thermocouples were calibrated against the freezing points of reagent grade Sn (231.9 °C) and NaCl (800.5 °C). A copper cup encased both the capsule and thermocouple tips to minimize thermal gradients in the vicinity of the sample. Loose refractory insulation was packed around the capsule and thermocouple along the entire length of the sample holder to minimize argon convection and provide a more uniform temperature in the sample holder. Uncertainties in temperature measurements cited for the internally heated experiments include error resulting from daily temperature fluctuations and estimated calibration errors.

Starting materials

The starting material for each experiment consisted of natural (tremolite and quartz) and synthetic (calcite, for-

TABLE 2. Experimental data for the equilibrium Tr + Fo = 2Di + 5En + H_2O

Experiment no.	T (°C)	P_{H_2O} (kbar)	Duration (h)	Results	Extent of reaction—XRD
20	684(3)	0.2	2040	Tr(+)Fo(+)Di(−)En(−)	W
19	696(4)	0.2	4417	Tr(+)Fo(+)Di(−)En(−)	W
18	708(2)	0.2	4078		None
4	710(5)	0.5	960	Tr(+)Fo(+)Di(−)En(−)	W-M
5	744(3)	0.5	1224	Tr(+)Fo(+)Di(−)En(−)	W-M
6	763(6)	0.5	811	Tr(+)Fo(+)Di(−)En(−)	SEM
7	781(7)	0.5	859	Tr(−)Fo(−)Di(+)En(+)	W
12	799(5)	0.5	1707	Tr(−)Fo(−)Di(+)En(+)	M-S
1	724(2)	1.0	1320	Tr(+)Fo(+)Di(−)En(−)	M-S
2	755(3)	1.0	1320	Tr(+)Fo(+)Di(−)En(−)	S
3	771(3)	1.0	1344	Tr(+)Fo(+)Di(−)En(−)	M
8	790(8)	1.0	624	Tr(+)Fo(+)Di(−)En(−)	W
17	809(3)	1.0	2088	Tr(+)Fo(+)Di(−)En(−)	W-M
21	820(4)	1.0	685	Tr(−)Fo(−)Di(+)En(+)	W
1-2*	822(3)	5.04	335	Tr(+)Fo(+)Di(−)En(−)	S
1-5*	833(4)	5.14	438	Tr(+)Fo(+)Di(−)En(−)	W
1-1*	842(4)	5.00	284	Tr(+)Fo(+)Di(−)En(−)	SEM
1-4*	852(4)	5.12	669	Tr(+)Fo(+)Di(−)En(−)	SEM
1-6*	858(4)	5.13	388		None
1-3*	870(4)	5.02	332	Tr(−)Fo(−)Di(+)En(+)	S

Notes: Growth or diminution of a phase is indicated by a (+) or (−), respectively. Symbols S, M, and W are qualitative estimates of the extent of reaction as judged by XRD and represent strong, moderate, and weak, respectively. SEM means reaction direction was judged by scanning electron microscope. See text for discussion of temperature uncertainty, which is given as ±2 standard deviations about the mean temperature.

* Experiments performed at Binghamton University. All other experiments performed at the University of Maine.

sterite, diopside, and enstatite) phases combined with excess H_2O or with excess supercritical H_2O-CO_2 fluid. The synthetic forsterite, diopside, and enstatite were prepared individually (described below) from mixtures having the bulk compositions $2MgO{\cdot}SiO_2$, $CaO{\cdot}MgO{\cdot}2SiO_2$, and $MgO{\cdot}SiO_2$, respectively. Calcium was weighed out as $CaCO_3$ (Fisher, lot 771134), SiO_2 glass was obtained from Corning (lump cullet 7940, lot 62221), and MgO was obtained from Fisher (lot 787699). SiO_2 glass and MgO were fired at 1000 °C for 2 to 3 hours, and $CaCO_3$ was heated at 200 °C for l week to drive off adsorbed H_2O. For investigating Equilibrium 1, stoichiometric proportions of tremolite + forsterite were mixed with an equal amount (by weight) of diopside + enstatite and homogenized by grinding under H_2O with an automatic mortar and pestle for 30 min to ensure fine grain size and consequent reactivity. This starting material was used in experiments conducted at both the University of Maine and Binghamton University.

Two different starting materials were used for reversing Equilibrium 4 for reasons discussed below. Starting material I contained stoichiometric proportions of tremolite + calcite + quartz mixed with diopside in a 60:40 ratio by weight. Starting material II was similar to starting material I but contained 5.6 wt% excess quartz. Starting materials I and II were homogenized by grinding under alcohol with an automatic mortar and pestle for 30 min.

Either oxalic acid or silver oxalate was used as a source of CO_2 in experiments bracketing Equilibrium 4. Blank experiments using only oxalic acid produced a fluid having $X_{CO_2} = 0.45$ rather than the theoretical $X_{CO_2} = 0.50$. Blank experiments using only silver oxalate produced a fluid containing 99% of the theoretical mass of CO_2.

Examination of experimental products

After the conclusion of an experiment, solids were gently disaggregated under acetone with an agate mortar and pestle. Although the experimental products were homogeneous, the interior of a charge generally appeared finer-grained than that portion of the sample in contact with the capsule wall. The products of each experiment were examined with polarized light microscopy (PLM), X-ray diffraction (XRD), and scanning electron microscopy (SEM). PLM proved useful for observing gross morphological changes that occurred during hydrothermal treatment. Unfortunately, the experimental products consisted of an intimate mixture of fine-grained phases, which precluded the establishment of reliable criteria for judging reaction direction with PLM.

Initially, XRD was used to determine reaction direction for Equilibria 1 and 4. Relative intensities of X-ray reflections of all phases in the high- and low-temperature assemblages in the starting materials were compared with

TABLE 3. Experimental data for the equilibrium Tr + 3 Cc + 2 Qz = 5 Di + 3 CO_2 + H_2O

Exper. No.	P_{fluid} (kbar)	T (°C)	Duration (h)	X_{CO_2} Initial	X_{CO_2} Final	Starting material	Results	Extent of reaction
9	5	577(3)	1506	0.69	0.71	I	Tr(+)Cc(+)Qz(−)Di(−)En(+)	M
16	5	586(4)	4032	0.20	0.22	I	Tr(+)Cc(+)Qz(−)Di(−)En(+)	S
21	5	601(5)	3617	0.45	0.53	II	Tr(+)Cc(+)Qz(−)Di(−)	S
8	5	605(3)	1510	0.71	0.73	I	Tr(+)Cc(+)Qz(−)Di(−)En(+)	W
7	5	626(2)	1338	0.70	0.73	I	Tr(−)Cc(−)Qz(−)Di(+)En(?)	W
30	5	631(3)	6333	0.50	0.53	II	Tr(−)Cc(−)Qz(−)Di(+)	S
31	5	653(5)	6333	0.45	0.50	II	Tr(−)Cc(−)Qz(−)Di(+)En(?)	S
32	5	673(4)	6313	0.52	0.56	II	Tr(−)Cc(−)Qz(−)Di(+)	S

Notes: Growth or diminution of a phase is indicated by a (+) or (−), respectively. Symbols S, M, and W are qualitative estimates of the extent of reaction as judged by XRD and represent strong, moderate, and weak, respectively. Starting material II contains excess quartz whereas starting material I contains a stoichiometric proportion of quartz. See text for discussion of temperature uncertainty, which is given as ±2 standard deviations about the mean temperature.

TABLE 4. Unit-cell parameters of phases used in the starting materials

Phase	*a* (Å)	*b* (Å)	*c* (Å)	β	*V* (Å³)	*S*	*N*
Enstatite	18.222(3)	8.822(1)	5.174(1)	—	831.85(15)	CaF_2	44
Diopside	9.745(2)	8.923(2)	5.253(1)	105°53′	439.32(10)	Si	47
Forsterite	4.751(1)	10.198(1)	5.979(1)	—	289.76(5)	CaF_2	42
Calcite	4.991(1)	—	17.072(4)	—	368.25(10)	BaF_2	21
Quartz*	4.9124(1)	—	5.4052(2)	—	112.96(6)	Si	13
Tremolite†	9.838(1)	18.049(2)	5.278(1)	104°45.1′(7)	nr	nr	nr

Notes: Figures in parentheses represent the estimated standard deviation in the last digit; the uncertainties were calculated using a unit-cell refinement program and represent precision only. Abbreviations: *S* = X-ray standard; *N* = number of reflections used in the refinement; nr = value not reported.
* Values determined by S. Huebner and K. Shaw.
† Values reported by Krupka et al. (1985).

relative intensities of X-ray reflections of corresponding phases in the products of each experiment. Provided that sufficient reaction has occurred, relative intensities of X-ray reflections of phases in the stable assemblage increase while relative intensities of X-ray reflections in the unstable assemblage decrease. Reaction rates for Equilibrium 4 were rapid enough to obtain tight brackets using XRD; however, sluggish reaction rates for Equilibrium 1 precluded obtaining tight brackets for this equilibrium with XRD.

An Amray 1000 SEM operated at 20 kV and equipped with an ORTEC energy dispersive spectrometer (EDS) was used as the primary tool to determine reaction direction for Equilibrium 1 and to confirm the XRD results for several experiments on Equilibrium 4. Lack of appropriate software precluded quantitative analysis with the EDS but did allow unambiguous identification of each phase.

We found it necessary to disaggregate the experimental products to optimize SEM observations. To disaggregate clusters of grains, approximately 2 mg of solids were combined with several cubic centimeters of methanol in a test tube and dispersed in an ultrasonic bath. The suspended finer-grained fraction (typically less than 3 mm) was aspirated onto a Cu tape glued to an Al SEM stub. Although this procedure greatly enhanced observation of fine grains, grains coarser than about 3 mm tended to settle and consequently were omitted from the mount. After allowing the coarser-grained fraction to settle, several drops of methanol containing this fraction were placed on Cu tape and allowed to dry. This procedure resulted in a mount containing coarse grains relatively free of adhering finer-grained particles. The edges of the Cu tape and Al stub were coated with silver paint and sputtered with gold to prevent ''charging'' of the sample. Approximately 30–50 grains in both the coarse-grained and fine-grained fractions of each sample were examined.

RESULTS

Characterization of phases used in the starting materials

Unit-cell parameters of phases used in the starting materials were calculated by refining powder patterns obtained with an Enraf-Nonius FR552 Guinier camera and Cu$K\alpha_1$ radiation. CaF_2 (Baker Lot 91458, a = 5.462 ± 0.005 Å) and BaF_2 (Baker Lot 308, a = 6.1971 ± 0.0002 Å) standardized against gem diamond (a = 3.56703 Å, Robie et al. 1967), as well as Si (NBS Standard Reference Material 640) were used as internal standards. Least squares unit-cell refinements were performed using the computer program of Appleman and Evans (1973).

Tremolite [$Ca_2Mg_5Si_8O_{22}(OH_2)$] from St. Gotthard, Switzerland was obtained from D. Kerrick. An analysis of this material was reported by Slaughter et al. (1975). The chemical analysis was performed on an optically pure sample using wet chemical and emission spectrographic techniques (D. Kerrick, personal communication) and indicates the presence of minor F (0.0.7 wt%), Fe_2O_3 (0.30 wt%), FeO (0.27 wt%), and excess Ca (0.16 cations per formula unit). Redetermination of the analysis was not possible due to the extremely fine-grained nature of the material obtained from D. Kerrick. A portion of this material was used in phase equilibrium studies by Slaughter et al. (1975) and Eggert and Kerrick (1981) and for high-temperature heat capacity measurements by Krupka et al. (1985). The cell parameters (Table 4) reported by Krupka et al. (1985) are very similar to those of natural tremolite (PDF 13-437 and 20-1310).

Diopside ($CaMgSi_2O_6$) was synthesized at l atm by fusing glass starting material at 1450 °C for 15 min, cooling to 1285 °C in 1 hour, and continued heating at this temperature for 12 hours. The glass starting material was prepared by fusing the $CaO{\cdot}MgO{\cdot}SiO_2$ mix described earlier (with CaO as $CaCO_3$) twice at 1450 °C followed by grinding to ensure homogeneity. The synthetic crystals were examined with a petrographic microscope and found to be inclusion free and optically homogeneous. The powder pattern and unit-cell parameters (Table 4) agree with those of natural diopside (PDF 112-654).

Calcite ($CaCO_3$) was obtained from Fisher Scientific (lot 771134). The powder pattern and unit-cell parameters (Table 4) compare favorably with those of synthetic calcite (PDF 5-586). Forsterite (Mg_2SiO_4) was synthesized hydrothermally at 800 to 815 °C, P_{H_2O} = 0.5 to 1 kbar in experiments of 5 to 20 days duration. Resultant crystallites are fine-grained (9 μm), anhedral, and contain a trace of an unidentified impurity. The powder pattern and unit-cell parameters (Table 4) are very close to those for synthetic forsterite (Fisher and Medaris 1969). Enstatite ($MgSiO_3$) was synthesized hydrothermally at P_{H_2O} = 1 kbar and temperatures ranging from 800 to 815 °C in 5

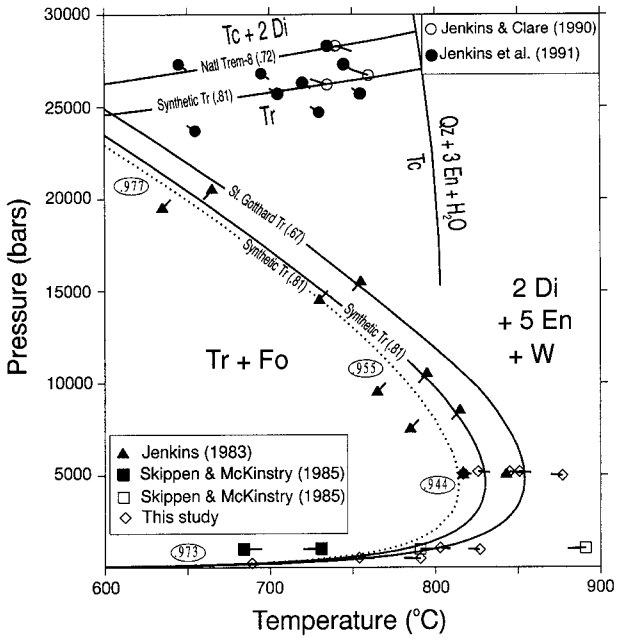

FIGURE 2. Experimental results for the equilibria Tr + Fo = 2Di + 5En + H_2O and Tr = Tc + 2Di, obtained using natural tremolite (open symbols) and synthetic tremolite (filled symbols). Curves were computed with newly derived thermodynamic data for hypothetical end-member tremolite (Table 6), ideal tremolite activities (shown in parentheses and in Table 5), and either end-member (solid curves) or predicted stable pyroxene compositions (dotted curve with X_{Di} values shown in the ovals). Note displacement of the latter to lower temperatures by up to 25 °C. The equilibrium Tr = Tc + 2Di is metastable above the euilibrium Tc = 3Qtz + En + H_2O.

to 14 days. The synthetic enstatite crystals are fine-grained (10 μm), prismatic, inclusion-free, commonly twinned, and exhibit parallel extinction. The unit-cell parameters are given in Table 4 and compare favorably with those of natural enstatite (PDF 22-714). Quartz (SiO_2) from Minas Gerais, Brazil, has unit-cell parameters (Table 4) that agree with those of quartz from Lake Toxaway, North Carolina (PDF 5-0490).

The equilibrium Tr + Fo = 2Di + 5En + H_2O

Results of experiments on this equilibrium are listed in Table 2 and plotted on Figure 2. Samples were prepared by sealing 7 to 11 mg of starting material together with excess H_2O in 1.25 cm long gold capsules. The mass of fluid at the initiation of an experiment varied from 6.4 to 7.6 mg; the mass of the solids ranged from 1.1 to 1.6 times greater than the mass of the fluid. Sufficient fluid was present to ensure that $P_{fluid} = P_{solids}$. Brackets were obtained at 5, 1, and 0.5 kbar and a low-temperature half-bracket at 0.2 kbar. Reaction rates at 0.2 kbar are very sluggish compared with reaction rates at 5 kbar. Although experiment no. 19 at 696 °C and 0.2 kbar lasted over 4400 hours, it proved to be a weak indicator of reaction direction; another experiment at 708 °C and 0.2 kbar did not indicate reaction direction after >4000 hours. By comparison, the 5 kbar bracket was established in fewer than 700 hours.

Initially, XRD was used to determine reaction direction. Those experiments where XRD proved useful are identified in Table 2. An experiment was considered successful if an estimated 30% change could be observed in the intensities of selected reflections of an experimental product relative to those of the starting material. Unfortunately, XRD data proved to be weak indicators of reaction direction in a number of experiments (Table 2), and they did not provide any useful information for several key experiments (6, 18, 1-1, 1-4, and 1-6) occurring close to the equilibrium curve.

Systematic SEM observation of all experimental products was undertaken to determine if the ''weak'' XRD signals could be confirmed as well as to determine if experiments that showed ''no reaction'' on XRD traces exhibited surface and/or textural features indicative of reaction direction. Grain size in the starting material ranged from 0.3–15 μm (Fig. 3a). Euhedral cleavage fragments of tremolite up to 15 μm long and subhedral enstatite laths up to 7 μm long were common in the starting material (Fig. 3a) whereas euhedral cleavage fragments of enstatite were rare. Forsterite and diopside grains tended to be equant and anhedral although some diopside grains had a subhedral blocky appearance.

It should be emphasized that not all grains gave a clear indication of growth or dissolution, and numerous grains had to be examined before reaction direction could be assigned confidently. In general, tremolite and enstatite grains most commonly displayed growth/dissolution features, whereas diopside (in a few cases) and forsterite (rarely) displayed growth/dissolution features.

Photomicrographs in Figures 3 and 4 illustrate the features used to judge reaction direction. On the low-temperature side of the equilibrium curve, tremolite grains most commonly displayed a prismatic habit with well-formed terminations (Fig. 3b) or a lath-shaped habit (Fig. 3c). Tremolite grains shown in Figures 3b and 3c did not nucleate on coarse tremolite seeds. Forsterite was generally rounded (Fig. 3c) and only rarely displayed crystal habit. Enstatite laths displayed rounded ends (Fig. 4a).

On the high-temperature side of the equilibrium curve, enstatite laths and prisms were euhedral with good terminations (Fig. 4b). Tremolite seeds appeared rounded and pitted (Fig. 4b) and small prisms of tremolite were absent.

Based on surface features similar to those illustrated above, three (6, 1-1, and 1-4) of the five experiments whose XRD traces showed ''no reaction'' were used to constrain the equilibrium curve. Growth and dissolution features in the other two experiments (18 and 1-6) were inconclusive.

Our results at 0.5, 1.0, and 5.0 kbar yield relatively tight brackets, between 10 and 20 °C, on Equilibrium 1. The new data are consistent with, but displaced to the low-temperature side of the rather wide bracket obtained

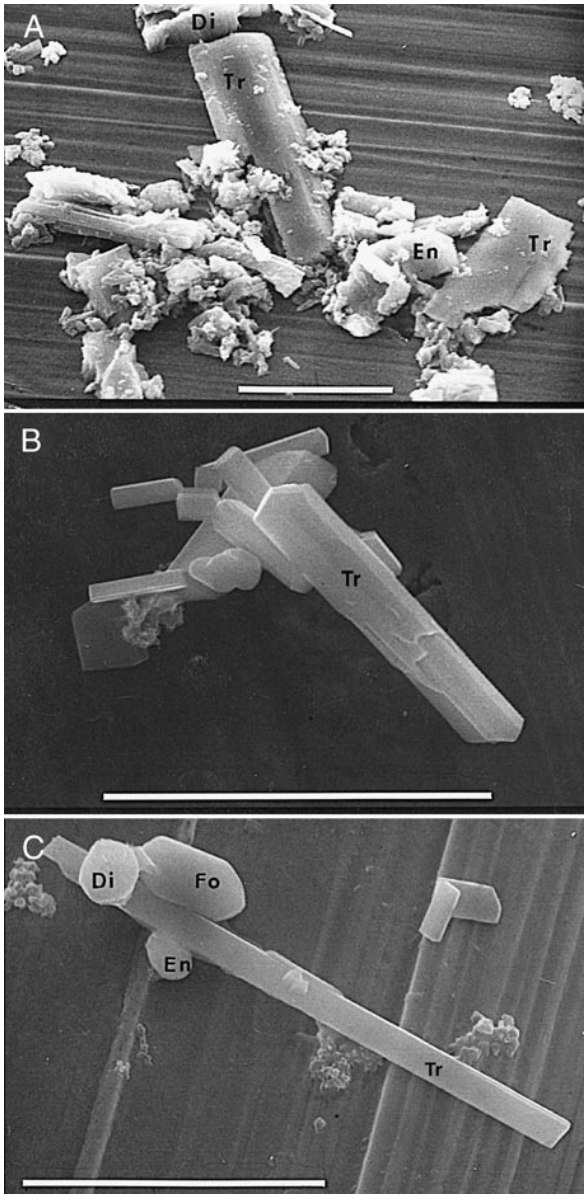

FIGURE 3. SEM photomicrographs showing (top) highly variable grain size in the starting material; (middle) prismatic tremolite that nucleated and grew in Experiment 1-5; and (bottom) lath-shaped tremolite that nucleated and grew in Experiment 1-1. Scale bar is 10 μm long in all figures.

for this equilibrium by Skippen and McKinstry (1985) when the same St. Gotthard tremolite (Fig. 2) was used in the starting material. The new bracket at 5 kbar lies about 25 °C above the bracket of Jenkins (1983), who used synthetic tremolite in his starting material, and is consistent with thermodynamic calculations described below that account for the compositional difference between synthetic and St. Gotthard tremolite. In comparison, the 1 kbar bracket that Skippen and McKinstry (1985) obtained using synthetic tremolite in their starting material lies approximately 50 °C below the computed curve for synthetic tremolite and about 40 °C below the temperature permitted by the data of Jenkins (1983).

The grain size (1–2 μm) of synthetic tremolite used by Skippen and McKinstry (1985) was considerably finer than the grain size of synthetic tremolite used in other studies. For example, Jenkins and Clare (1990) reported an average grain size of 13 × 2 μm, achieved through a two-step synthesis procedure. This comparison suggests that the tremolite of Skippen and McKinstry may have been poorly crystalline, and thus less stable, despite synthesis times of 28–42 days. Another possibility, that reaction direction was misinterpreted, is not possible to evaluate because extents of reaction for each half-bracket were not tabulated, but the reported minimum of 10% relative change in XRD peak intensities is low.

The equilibrium Tr + 3Cc + 2Qtz = 5Di + H_2O + 3CO_2

Results of experiments on the equilibrium Tr + 3Cc + 2Qtz = 5Di + H_2O + 3CO_2 are listed in Table 3 and plotted on Figure 5. Samples were prepared by sealing 6 to 12 mg of starting material together with oxalic acid for Experiment 21 or silver oxalate + H_2O for all other experiments. The mass of fluid at the initiation of an experiment ranged from 4.4 to 7.1 mg and the mass of the solids was 0.98 to 1.8 times greater than the mass of the fluid. Sufficient fluid was present to ensure that $P_{fluid} = P_{solids}$. The experiments were of sufficient duration to ensure that samples in the gold capsules were buffered at or near Ni-NiO by the vessel wall (Huebner 1971). Hence, we assume that the fluid phase is essentially a binary H_2O-CO_2 mixture (Kerrrick 1974).

As is typical of equilibria involving amphiboles, reaction rates are sluggish and several experiments over 6000 hours in duration were required to establish reaction direction. In addition, the consumption of quartz (even when the low-temperature assemblage was stable) as well as the growth of a few percent of enstatite in some of the experiments (Table 3) indicates that a competing reaction occurred.

The (101) reflection of quartz at d = 3.343 Å was missing only from the XRD trace of experiment 16; hence μ_{SiO_2} was fixed in all other experiments. The presence of enstatite in the experiments listed in Table 3 was inferred from the presence of the very weak (420) reflection at d = 3.18 Å; forsterite reflections were not observed. Our observations support the conclusion of Jenkins (1987) that hydrothermal treatment of natural tremolite in mildly silica-undersaturated fluids could result in its incongruent dissolution by the equilibrium

$$\text{Tr} = \text{En} + \text{Di} + \text{SiO}_2(\text{aq}) + \text{H}_2\text{O}.$$

Despite the uncertainties mentioned above, a fairly tight bracket was obtained at P_{fluid} = 5 kbar and X_{CO_2} = 0.73. Our bracket at P_{fluid} = 5 kbar lies about 25 °C below the bracket obtained by Slaughter et al. (1975), who also used St. Gotthard tremolite in the starting material. Although these authors used three techniques (single-crystal

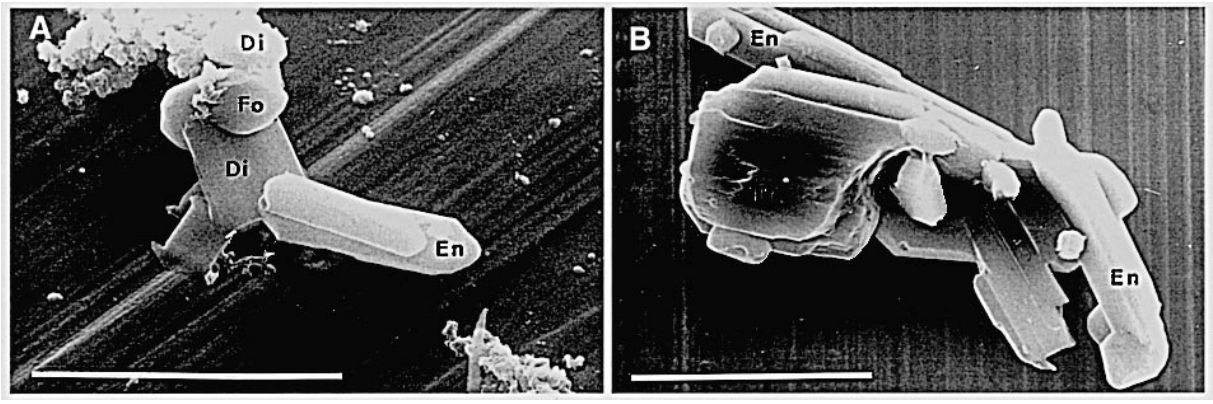

FIGURE 4. SEM photomicrographs showing (left) rounded subhedral enstatite prisms and rounded diopside and forsterite grains produced during Experiment 1-4; (right) euhedral enstatite prisms, and laths and a partially dissolved tremolite seed produced during Experiment 1-3. Scale bar is 10 μm long in both figures.

weight change experiments, all-powder experiments, and atomic absorption analyses of carbonates in experimental products) to determine reaction direction, their experiments were of shorter duration than ours (500 vs. 1338–6333 hours). Slaughter et al. (1975) did not cite evidence for a competing reaction that consumed quartz but, if such a reaction did occur in their weight change experiments, it might account for the three ''low-temperature'' reversals that are discrepant with our new data (Fig. 5).

Our new bracket lies at approximately the same temperature as the data Metz (1983) obtained with synthetic tremolite (Fig. 5). This overlap is consistent with thermodynamic calculations summarized below that indicate a 5 °C increase in the position of this equilibrium with St. Gotthard vs. synthetic tremolite.

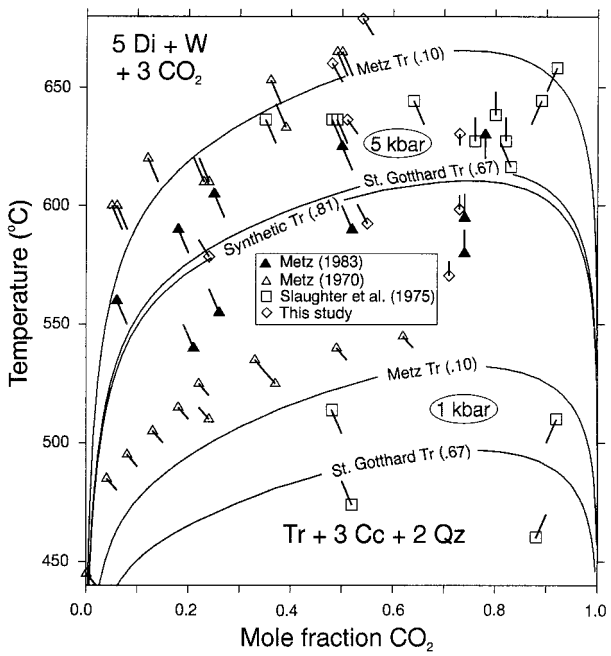

FIGURE 5. Experimental results for the equilibrium Tr + 3Cc + 2Qz = 5Di + H_2O + 3CO_2. Experimental data are from this study (St. Gotthard tremolite), Metz (1970; Campo Longo tremolite), Slaughter et al. (1975; St. Gotthard tremolite), and Metz (1983; synthetic tremolite). Curves were computed with newly derived thermodynamic data for hypothetical end-member tremolite (Table 6), ideal tremolite activities (shown in parentheses and in Table 5), and end-member pyroxene compositions.

Thermodynamic analysis

On the basis of experimental data for Equilibria 2 and 3, Jenkins and Clare (1990) concluded that the observed differences in positions of these equilibria obtained using natural and synthetic tremolites in the starting materials could be reconciled by the compositional differences among these tremolites. Table 5 summarizes the structural formulae of the tremolites used by Jenkins and Clare (1990) as well as the tremolites used in all other experimental studies. It should be noted that the tabulated formulae for TREM-8 (Jenkins and Clare 1990) and St. Gotthard (Slaughter et al. 1975) tremolites were computed on the basis of 23 O atoms (H_2O analyses are not available) and differ from previously published structural formulae. The formula for Campo Longo tremolite is also based on 23 O atoms because the H_2O content (Metz 1967) and fluorine content (Metz, personal communication) yield OH + F > 2 (= 2.54). Table 5 shows tremolite activities, computed with the cation occupancy scheme of Leake (1978) and ideal site mixing equations, that are used below in thermodynamic calculations. For the Campo Longo tremolite, we used the activity based on the more recent fluorine analysis.

The composition assigned to synthetic tremolite is based on the work of Jenkins (1987), which suggests that synthetic tremolite contains 10 ± 3 mol% Mg on the M4 site. A similar assumption also was made by Jenkins and Clare (1990), Jenkins et al. (1991), and Pawley et al. (1993). Maresch et al. (1994), on the other hand, proposed that chain multiplicity faults, recognized in syn-

TABLE 5. Compositions of tremolites used in experimental studies

Locality (name)	Composition	Activity
Hypothetical end-member	$Ca_2Mg_5Si_8O_{22}(OH)_2$	1.00
Synthetic	$Ca_{1.8}Mg_{5.2}Si_8O_{22}(OH)_2$	0.81
St. Gotthard	$(K_{0.01}Na_{0.01})Ca_{2.16}Mg_{4.94}Si_{7.92}O_{22}(OH)_{1.97}F_{0.03}$	0.67
Ontario (TREM-12)	$(K_{0.04}Na_{0.16})Ca_{1.91}Mg_{4.96}Si_{7.93}O_{22}(OH)_{1.8}F_{0.21}$*	0.56
Massachusetts (TREM-8)	$(K_{0.01}Na_{0.05})Ca_{1.97}Mg_{4.98}Si_{7.94}O_{22}(OH)_{1.85}F_{0.09}$	0.72
Welch and Pawley (1992) tremolite	$Ca_{1.98}Mg_{5.06}Si_{7.95}O_{22}(OH)_{1.98}$	0.91
Campo Longo	$(K_{0.07}Na_{0.11})Ca_{1.72}Mg_{5.18}Si_{7.85}O_{22}(OH)_{1.52}F_{1.02}$	0.30 (0.10)†

Notes: St. Gotthard analysis obtained by wet chemical and emission spectrographic techniques; other natural amphibole compositions based on reported electron microprobe analyses. Synthetic tremolite composition (Jenkins 1987) obtained by electron microprobe analysis. Activity computed using site occupancy scheme of Leake (1968):

for $Ca > 2$ $a_{Tr} = (3\text{-}Ca\text{-}Na\text{-}K)(X_{Ca})^2(X_{Mg})^5(X_{Si})^8(X_{OH})^2$ (Skippen and Carmichael 1977)

for $Ca < 2$ $a_{Tr} = (1\text{-}Na\text{-}K)(X_{Ca})^2(X_{Mg})^5(X_{Si})^8(X_{OH})^2$.

* OH content determined as 2-F content.

† Value in parentheses based on F analysis (see text).

thetic products by HRTEM analysis, account for the lower than ideal Ca/Mg ratio of synthetic tremolite. They suggested that synthetic tremolite-rich intergrowths are energetically comparable to discrete stoichiometric tremolite crystals. The success in the present study of extracting consistent thermodynamic properties for both natural and synthetic tremolite (see below) assuming the latter to contain 10 mol% magnesiocummingtonite component can be taken as either support for the validity of this assumption or as an indication that chain multiplicity faults in tremolite produce a similar degree of stabilization as this solid solution.

To refine thermodynamic properties for tremolite, mathematical programming analysis (MAP; Berman et al. 1986) was performed using 23 data sets involving the 11 tremolite-bearing equilibria that have been experimentally investigated (Table 1). With this technique, each experimental datum, adjusted for experimental uncertainties, is treated as an inequality constraining the Gibbs free energy change of the reaction. For each data set, fixed tremolite activities (Table 5) were used to account for the measured compositions of tremolite samples used in these experiments. To account for calibration errors in the experiments performed at the University of Maine (Tables 2 and 3), 3 °C was added to the tabulated temperature uncertainties, which only include variability due to daily temperature fluctuation. The results yield thermodynamic properties of hypothetical, stoichiometric tremolite, which provide the most sound basis for applications to natural samples.

Thermodynamic data for all phases other than tremolite, anthophyllite, and talc were fixed at the values given by Berman (1988). The entropy of tremolite was constrained by the calorimetric measurements on Falls Village, Connecticut, tremolite (Robie and Stout 1963). Although Robie and Stout did not report the F content of this tremolite, microprobe data obtained in this study on a sample provided by R.A. Robie indicate that F is below detection limits (<0.1 wt%).

The molar volume of stoichiometric tremolite was constrained between 27.245 and 27.298 J/bar, values obtained from a low cummingtonite natural tremolite, CG-1. The first value was obtained by powder XRD (Welch and Pawley 1991) and was used by these investigators for phase equilibrium and calorimetric study. The second value is the higher of two single-crystal measurements reported by Yang and Evans (1996). Although the analysis of this sample by Welch and Pawley (1991) suggests about 5.5% cummingtonite, the analysis by Yang and Evans (1996) indicates only about 1% cummingtonite. The molar volume determined by Borg and Smith (1969) for sample G-21 from Gouverneur, New York, which has approximately 4.1% cummingtonite based on the analysis given by Ross et al. (1969), is slightly lower (27.225 J/bar) than the values used in our computations.

Thermodynamic properties of anthophyllite and talc were constrained by the same $MgO\text{-}SiO_2\text{-}H_2O$ phase equilibrium data and thermophysical data summarized by Berman (1988), with the following exceptions. The molar volume of anthophyllite was taken from the detailed assessment of Hirschmann et al. (1994). Thermal expansivity and compressibility terms for talc and tremolite were constrained by thermophysical data summarized by Berman (1988) and recent compressibility measurements for tremolite (Comodi et al. 1991). Final values were obtained through MAP optimization using phase equilibrium data for Equilibrium 3 as well as the high-pressure bracket for the equilibrium

$$Tc = En + Qz + H_2O$$

reported by Jenkins et al. (1991). This bracket is about 40 °C higher than a preliminary bracket obtained for this equilibrium by T.J.B. Holland (personal communication to Chernosky). The resulting thermodynamic properties (Table 6) also reproduce the extremely tight brackets (~5 °C) for this equilibrium between 2–10 kbar obtained by Aranovich and Newton (unpublished results).

A major complication in retrieving thermodynamic properties for tremolite from equilibria involving clinopyroxene stems from the significant variation in Cpx composition with pressure, temperature, and different mineral assemblage. Jenkins et al. (1991) assumed constant Cpx ($X_{Di} = 0.95$) and Opx ($X_{En} = 0.99$) compositions given by the model of Lindsley (1983) for coexist-

TABLE 6. Standard state thermodynamic properties of minerals (at 1 bar and 298.15 K) modified from Berman (1988)

Mineral	ΔH^o (J/mol)	S^o (J/mol)	V (J/bar)	v_1 ($\times 10^6$)	v_2 ($\times 10^{12}$)	v_3 ($\times 10^6$)	v_4 ($\times 10^{10}$)
Anthophyllite	−12073.26	535.13	26.3300	−1.139	0.000	28.105	62.894
Talc	−5897.69	260.91	13.6100	−1.847	5.878	25.616	0.000
Tremolite	−12305.48	549.86	27.2950	−1.421	8.536	22.742	116.505

Notes: Anthophyllite $C_p = 1233.79 - 71.34\ T^{-1/2} - 221.638\ T^{-2} + 233.394\ T^{-3}$ (J/mol·K). Volume: $V^{P,T}/V^{1,298} = 1 + v_1\ (P\text{-}1) + v_2\ (P\text{-}1)^2 + v_3\ (T\text{-}298) + v_4\ (T\text{-}298)^2$ (Berman 1988).

ing pyroxenes, and they concluded that accounting for these solid solutions and nonstoichiometry in synthetic tremolite leads to a tremolite enthalpy 900 J less stable compared to calculations based on pure phases. In this study, we used the solution model of Davidson et al. (1988) and the free energy minimization software THERIAK (de Capitani and Brown 1987) to predict pyroxene compositions over the *P-T* range of all experimentally studied equilibria. The greatest amount of solid solution occurs at the highest temperatures achieved in Equilibria 2 and 1, with Cpx compositions changing with increasing T from $X_{Di} = 0.978$ to 0.903 and 0.973 to 0.935, respectively (Figs. 6 and 2), over the temperature range of the available experiments. Opx compositions range from $X_{En} = 0.998$ to 0.976 for Equilibrium 2 and from $X_{En} = 0.998$ to 0.987 for Equilibrium 1. For Equilibrium 3, X_{Di} ranges from 0.994 at 600 to 0.961 at 800 °C (Fig. 2). For Equilibrium 4, $X_{Di} > 0.99$ at all *P-T* conditions. Accounting for the above pyroxene solid solutions lowers the temperature of Equilibria 1 and 2 by about 10 °C at 600 °C and by about 25 °C at 850 °C relative to calculations with stoichiometric end-member pyroxenes.

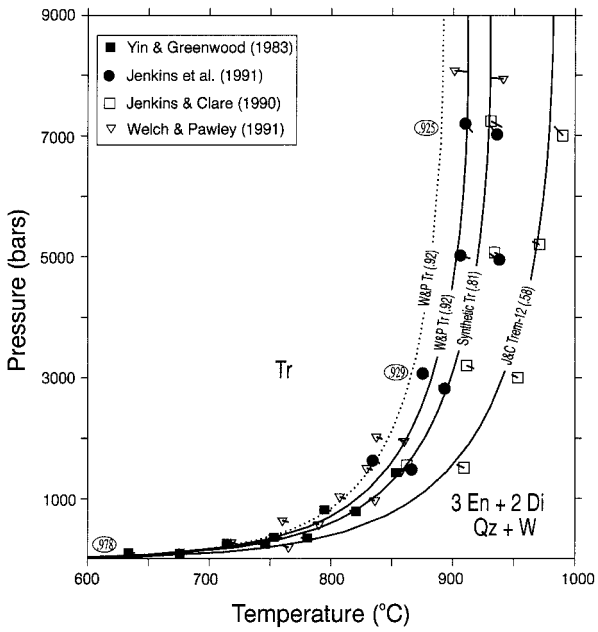

FIGURE 6. Experimental data for the equilibrium Tr = 3En + 2Di + Qz + H_2O using synthetic (filled symbols) and natural (open symbols) tremolites. Curves were computed with newly derived thermodynamic data for hypothetical end-member tremolite (Table 6), ideal tremolite activities (shown in parentheses and in Table 5), and either end-member (solid curves) or predicted stable pyroxene compositions (dotted curve with X_{Di} values shown). Note displacement of latter to lower temperature by up to 25 °C.

MAP analysis was performed on the combined data set involving natural and synthetic tremolite, using three different assumptions regarding pyroxene compositions: (1) metastable end-member pyroxenes in all starting materials persisted throughout all experiments; (2) stable pyroxene compositions formed early and therefore controlled tremolite stability in all experiments; and (3) tremolite grew relative to metastable end-member pyroxenes on the low-*T* side of the equilibrium boundary computed for end-member pyroxenes, whereas stable pyroxene compositions were achieved in experiments showing pyroxene growth on the high-*T* side of the equilibrium boundary. The latter assumption can be easily explored with MAP by processing all low- and high-*T* half-brackets with either end-member or stable pyroxene compositions, respectively.

Calculations with either assumption 1 or 2 produce 4–6 inconsistencies ranging in magnitude from 3–15 °C. With assumption 1, experiment no. 17 of this study forces tremolite to be more stable than allowed by the high-*T* reversals of Welch and Pawley (1991) and Yin and Greenwood (1983). Calculations based on assumption 2 lead to a tremolite enthalpy that is more stable by approximately 1.65 kJ/mol relative to calculations assuming pyroxenes are pure end-member Di and En. This added stability leads to contradictions with several sets of 500–600 °C mixed volatile experiments (Eggert and Kerrick 1981; Chernosky and Berman 1988), in which St. Gotthard tremolite was used and in which the predicted Cpx composition is very close to end-member Di (>0.99 X_{Di}).

Only the results with assumption 3 allowed consistency to be obtained with the large majority of experiments involving both synthetic and natural tremolite. Derived thermodynamic properties are given in Table 6, and calculated results for the five equilibria with the most experimental data are shown in Figures 2, 5, 6, and 7. All experimental data involving synthetic tremolite are mutually compatible, with the exception of the bracket for Equilibrium 1 reported by Skippen and McKinstry (1985), as discussed above. The experimental data involving natural tremolite are compatible among themselves and with the data for synthetic tremolite, with the following exceptions. Although the 1 kbar data of Slaugh-

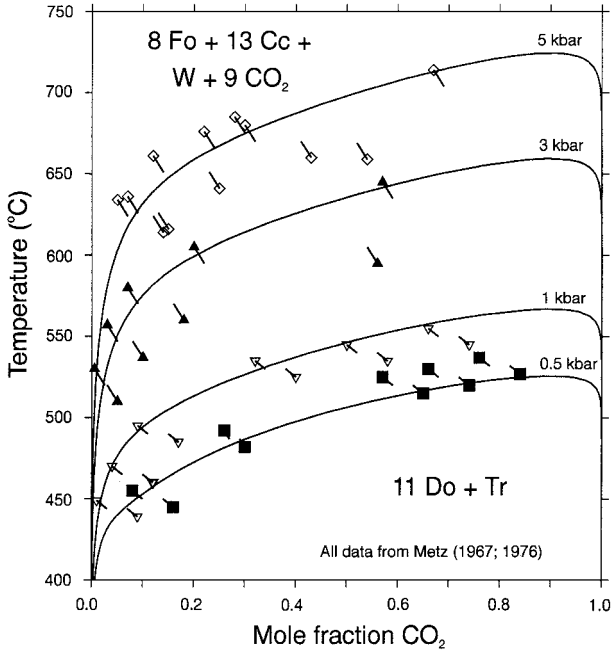

FIGURE 7. Experimental data of Metz (1967, 1976) for the Equilibrium 11Do + Tr = 8Fo + 13Cc + 9CO_2 + H_2O using Campo Longo tremolite. Computed curves as in Figure 5.

ter et al. (1975) for Equilibrium 4 discussed above are consistent with our calculations, their 5 kbar data are displaced to higher temperatures than our new experimental data using the same St. Gotthard tremolite (Fig. 5) and to about 30 °C higher temperature than our calculated curve. The two low-temperature half-brackets of Metz (1970) for the same equilibrium at l kbar (Fig. 5) are about 15 °C higher than that computed with the reduced activity (Table 5) for Campo Longo tremolite. As his data at 5 kbar (Fig. 5) are in good agreement with the calculated curves, the origin of this discrepancy is not clear. Last, a discrepancy of 8 °C occurs with one high-*T* half-bracket of Chernosky and Berman (1988) for the equilibrium:

$$\text{Tr} + \text{Cc} = \text{Fo} + \text{Di} + \text{H}_2\text{O} + \text{CO}_2 \qquad (10)$$

This experiment conflicts with experiment no. 17 of this study, regardless of which of the three assumptions are used in the data processing. Considering that both experiments were performed with St. Gotthard tremolite, error in its calculated activity cannot be a contributing cause of this incompatibility.

DISCUSSION

The new experiments presented in this study with St. Gotthard tremolite confirm the position of Equilibrium 1 determined by Skippen and McKinstry (1985), although our brackets define the position of this equilibrium near the low-temperature side of their rather wide bracket. Our data for Equilibrium 4 indicate approximately 25 °C lower temperatures than determined by Slaughter et al. (1975). Our thermodynamic analysis of the new data along with all other data sets involving both natural and synthetic tremolite offers strong confirmation of the assertion of Jenkins and Clare (1990) that tremolite compositional differences, accounted for with ideal on-site mixing, lead to the different *P-T* stabilities determined in these various studies. Stoichiometric tremolite breaks down by Equilibria 1 and 2 at temperatures approximately 25 °C lower than synthetic, Mg-enriched, tremolite. Although structural defects (Ahn et al. 1991; Maresch et al. 1994) undoubtedly raise the Gibbs free energy of synthetic relative to natural tremolite, the analysis presented above suggests that this factor is energetically of minor importance, with substantially less effect than differences in composition.

Our analysis suggests that observation of tremolite growth in experiments probably occurs relative to the metastable end-member pyroxenes used in all starting materials, rather than to the computed stable pyroxene compositions. On the other hand, pyroxene-stable half-brackets probably involve growth of pyroxenes with near-equilibrium compositions. This conclusion is compatible with the dissolution-reprecipitation mechanism presumed to be operational in these hydrothermal experiments, and it is supported by experimental observations of Lykins and Jenkins (1992). They found a somewhat larger stability field (~10 °C) for pargasite + Opx relative to plagioclase + Cpx + Fo + H_2O when metastable end-member anorthite, albite, and diopside were used in starting materials as compared to plagioclase (An50), Cpx, and Fo formed in a previous dehydration experiment.

The process envisioned here also may account for conflicting features seen in SEM analyses of some experiments that appear to be close to the Tr + Fo breakdown reaction. In experiment no. 17, for example, some euhedral tremolite laths and prisms suggest Tr + Fo stability, but most laths show small surface embayments that may indicate Tr + Fo instability. We suggest that in this experiment tremolite grew early after dissolution of metastable end-member pyroxenes, but that stable pyroxenes later grew at the expense of tremolite. Further work, both measuring the compositions of experimental products and performing experiments with stable and metastable starting materials, is needed to test our hypothesis.

The present analysis of all experimental data yields thermodynamic data at 1 bar and 298.15 K for hypothetical end-member tremolite that provide the most reasonable basis both to model the stability relations of natural amphiboles and to calibrate and apply amphibole thermobarometers. An important conclusion stemming from the analysis presented above is that broad agreement can be obtained between experiments performed with both natural and synthetic tremolite if one takes into account (1) minor compositional differences between the tremolites and (2) metastable tremolite growth with respect to non-equilibrium pyroxene compositions used in the experimental starting mixtures. One implication that needs to be verified with additional experimental work is that the upper stability of tremolite in nature may be approx-

imately 25 °C lower than previously inferred from the positions of experimental data using metastable pyroxene compositions.

Acknowledgments

D.M. Kerrick and R.A. Robie are gratefully acknowledged for providing natural tremolites from St. Gotthard, Switzerland and from Falls Village, Connecticut, respectively. We thank Paul Metz for providing an unpublished fluorine analysis of his Campo Longo tremolite. SEM observations were performed in the electron microscopy laboratory in the Department of Zoology at the University of Maine; SEM work could not have been completed without the cheerful help and advice of Kelley Edwards. D.M.J. gratefully acknowledges the generous support of the National Science Foundation (grant no. EAR-8507752). Perceptive reviews by G.B. Skippen and A.R. Pawley markedly improved this contribution and are gratefully acknowledged. This is Geological Survey of Canada contribution no. 64294.

References cited

Ahn, J.H., Cho, M., Jenkins, D.M., and Buseck, P.R. (1991) Structural defects in synthetic tremolitic amphiboles. American Mineralogist, 76, 1811–1823.

Appleman, D.E. and Evans, H.T. Jr. (1973) Job 9214: Indexing and least-squares refinement of powder diffraction data. United States National Technical Information Service, PB2-16188.

Berman, R.G. (1988) Internally-consistent thermodynamic data for stoichiometric minerals in the system Na_2O-K_2O-CaO-MgO-FeO-Fe_2O_3-Al_2O_3-SiO_2-TiO_2-H_2O-CO_2. Journal of Petrology, 29, 445–522.

Berman, R.G., Engi, M., Greenwood, H.J., and Brown, T.H. (1986) Derivation of internally-consistent thermodynamic data by the technique of mathematical programming, a review with application to the system Mg0-Si0_2-H_2O. Journal of Petrology, 27, 1331–1364.

Blundy, J.D. and Holland, T.J.B. (1990) Calcic amphibole equilibria and a new amphibole-plagioclase geothermometer. Contributions to Mineralogy and Petrology, 104, 208–224.

Borg, I.Y. and Smith, D.K. (1969) Calculated X-ray powder patterns for silicate minerals. Geological Society of America, Memoir 122.

Boyd, F.R. (1959) Hydrothermal investigations of amphiboles. In P.H. Abelson, Ed., Researches in geochemistry, p. 377–396. Wiley, New York.

Chernosky, J.V. Jr. and Berman, R.G. (1988) The stability of Mg-chlorite in supercritical H_2O-CO_2 fluids. American Journal of Science, 288-A, 393–420.

Comodi, P., Mellini, M., Ungaretti, L., and Zanazzi, P.F. (1991) Compressibility and high pressure structure refinement of tremolite, pargasite, and glaucophane. European Journal of Mineralogy, 3, 485–500.

Davidson, P., Lindsley, D., and Carlson, W. (1988) Thermochemistry of pyroxenes on the join $Mg_2Si_2O_6$-$CaMgSi_2O_6$: A revision of the model for pressures up to 30 kbar American Mineralogist, 73, 1264–1266.

de Capitani, C. and Brown, T.H. (1987) The computation of chemical equilibrium in complex systems containing non-ideal solutions. Geochimica Cosmochimica Acta, 51, 2639–2652.

Eggert, R.G. and Kerrick, D.M. (1981) Metamorphic equilibria in the siliceous dolomite system: 6 kbar experimental data and geologic implications. Geochimica et Cosmochimica Acta, 45, 1039–1049.

Evans, B.W. (1990) Phase relations of epidote-blueschists. Lithos, 25, 3–23.

Fisher, G.W. and Medaris, L.G. Jr. (1969) Cell dimensions and X-ray determinative curve for synthetic Mg-Fe olivines. American Mineralogist, 54, 741–753.

Gottschalk, M. (1994) Tremolite-tschermakite solid solutions; synthesis of large crystals and maximum tschermakite content as a function of paragenesis. Geological Society of America Abstracts with Programs, 26, 290.

Hewitt, D.A. (1975) Stability of the assemblage phlogopite-calcite-quartz. American Mineralogist, 60, 391–397.

Hirschmann, M., Evans, B.W., and Yang, H. (1994) Composition and temperature dependence of Fe-Mg ordering in cummingtonite-grunerite as determined by X-ray diffraction. American Mineralogist, 79, 862–877.

Holland, T.J.B. and Blundy, J.D. (1994) Non-ideal interactions in calcic amphiboles and their bearing on amphibole-plagioclase thermometry. Contributions to Mineralogy and Petrology, 116, 433–447.

Holland, T.J.B. and Powell, R. (1990) An enlarged and updated internally consistent thermodynamic dataset with uncertainties and correlations: The system K_2O-Na_2O-CaO-MgO-MnO-FeO-Al_2O_3-TiO_2-SiO_2-C-H_2-O_2. Journal of Metamorphic Geology, 8, 89–124.

Holloway, J.R. (1971) Internally heated pressure vessels. In G.C. Ulmer, Ed., Research techniques for high pressure and high temperature, p. 217–258. Springer-Verlag, New York.

Hoschek, G. (1973) Die Reaktion Phlogopit + Calcit + Quarz = Tremolit + Kalifeldspat + H_2O + CO_2. Contributions to Mineralogy and Petrology, 39, 231–237.

Huebner, J.S. (1971) Buffering techniques for hydrostatic systems at elevated pressures. In G.C. Ulmer, Ed., Research techniques for high pressure and high temperature, p. 123–177. Springer-Verlag, New York.

Jenkins, D.M. (1983) Stability and composition relations of calcic amphiboles in ultramafic rocks. Contributions to Mineralogy and Petrology, 83, 375–384.

———(1987) Synthesis and characterization of tremolite in the system H_2O-CaO-MgO-SiO_2. American Mineralogist, 72, 707–715.

Jenkins, D.M. and Clare, A.K. (1990) Comparison of the high-temperature and high-pressure stability limits of synthetic and natural tremolite. American Mineralogist, 75, 358–366.

Jenkins, D.M., Holland, T.J.B., and Clare, A.K. (1991) Experimental determination of the pressure-temperature stability field and thermochemical properties of synthetic tremolite. American Mineralogist, 76, 458–469.

Kerrick, D.M. (1974) Review of metamorphic mixed-volatile (H_2O-CO_2) equilibria. American Mineralogist, 59, 729–762.

Kohn, M.J. and Spear, F.S. (1989) Empirical calibration of geobarometers for the assemblage garnet + hornblende + plagioclase + quartz. American Mineralogist, 74, 77–84.

———(1990) with applications to southeastern Vermont. American Mineralogist, 75, 89–96.

Krupka, K.M., Hemingway, B.S., Robie, R.A., and Kerrick, D.M. (1985) High-temperature heat capacities and derived thermodynamic properties of anthophyllite, diopside, dolomite, enstatite, bronzite, talc, tremolite, and wollastonite. American Mineralogist, 70, 261–271.

Lamb, W.M. and Valley, J.W. (1988) Granulite facies amphibole and biotite equilibria, and calculated peak-metamorphic water activities. Contributions to Mineralogy and Petrology, 100, 349–360.

Leake, B. (1978) Nomenclature of amphiboles. American Mineralogist, 63, 1023–1052.

Lindsley, D.H. (1983) Pyroxene thermometry. American Mineralogist, 68, 477–493.

Lykins, R.W. and Jenkins, D.M. (1992) Experimental determination of pargasite stability relations in the presence of orthopyroxene. Contributions to Mineralogy and Petrology, 112, 405–413.

Mader, U.K. and Berman, R.G. (1992) Amphibole thermobarometry: a thermodynamic approach. Current research, Part E, Geological Survey of Canada Paper 92-1E, 393–400.

Mader, U.K., Percival, J.A., and Berman, R.G. (1994) Thermobarometry of garnet-clinopyroxene-hornblende granulites from the Kapuskasing structural zone. Canadian Journal of Earth Sciences, 31, 1134–1145.

Maresch, W.V., Czank, M., and Schreyer, W. (1994) Growth mechanisms, structural defects, and composition of synthetic tremolite: what are the effects on macroscopic properties? Contributions to Mineralogy and Petrology, 118, 297–313.

McKinstry, B.W. and Skippen, G. (1978) An experimental study of the stability of tremolite. Geological Society of America Abstracts with Program, 10, 454.

Metz, P. (1967) Experimentelle bildung von forsterit und calcit aus tremolit und dolomit. Geochimica et Cosmochimica Acta, 31, 1517–1532.

———(1970) Experimentelle untersuchung der metamorphose von kieselig dolomitischen sedimenten II. Die bildungsbedingungen des diopsids. Contributions to Mineralogy and Petrology, 28, 221–250.

———(1976) Experimental investigation of the metamorphism of siliceous dolomites III. Equilibrium data for the reaction: 1 tremolite + 11 dolomite = 8 forsterite + 13 calcite + 9 CO_2 + 11 H_2O for the total

pressures of 3000 and 5000 bars. Contributions to Mineralogy and Petrology, 58, 137–148.

———(1983) Experimental investigation of the stability conditions of petrologically significant calc-silicate assemblages observed in the Damara Orogen. In H. Martin and F.W. Eder, Eds., Intracontinental fold belts, p. 785–793. Springer-Verlag, New York.

Pawley, A.R., Graham, C.M., and Navrotsky, A. (1993) Tremolite-richterite amphiboles: Synthesis, compositional and structural characterization, and thermochemistry. American Mineralogist, 78, 23–35.

Puhan, D. and Metz, P. (1987) Experimental equilibrium data for the reactions 3 dolomite + 4 quartz + 1 H_2O = 1 talc + 3 calcite + 3 CO_2 and 5 talc + 6 calcite + 4 quartz = 3 tremolite + 6 CO_2 + 2 H_2O at a total gas pressure of 5000 bars. Neues Jahrbuch der Mineralogie Monatshefte, 11, 515–520.

Robie, R.A. and Stout, J.W. (1963) Heat capacity from 12 to 305 K and entropy of talc and tremolite. Journal of Physics and Chemistry, 67, 2252–2256.

Robie, R.A., Bethke, P.M., and Beardsley, K.M. (1967) Selected x-ray crystallographic data, molar volumes, and densities of minerals and related substances. U.S. Geological Survey Bulletin, 1248, 87 p.

Ross, M. Papike, J.J., and Shaw, K.W. (1969) Exsolution textures in amphiboles as indicators of subsolidus thermal histories. Mineralogical Society of America Special Paper 2, 275–299.

Skippen, G. (1971) Experimental data for reactions in siliceous marbles. Journal of Geology, 79, 457–481.

Skippen, G.B. and Carmichael, D.M. (1977) Mixed volatile equilibria. In H.J. Greenwood, Ed., Applications of thermodynamics to petrology and ore deposits, p. 109–125. Mineralogical Association of Canada.

Skippen, G. and McKinstry, B.W. (1985) Synthetic natural tremolite in equilibrium with forsterite, enstatite, diopside, and fluid. Contributions to Mineralogy and Petrology, 89, 256–262.

Skogby, H. and Ferrow, E. (1989) Iron distribution and structural order in synthetic calcic amphiboles studied by Mössbauer spectroscopy and HRTEM. American Mineralogist, 74, 360–366.

Slaughter, J., Kerrick, D.M., and Wall, V.J. (1975) Experimental and thermodynamic study of equilibria in the system CaO-MgO-SiO_2-H_2O-CO_2. American Journal of Science, 275, 143–162.

Troll, G. and Gilbert, M.C. (1972) Fluorine-hydroxyl substitution in tremolite. American Mineralogist, 57, 1386–1403.

Welch, M.D. and Pawley, A.R. (1991) Tremolite: New enthalpy and entropy data from a phase equilibrium study of the reaction tremolite = 2 diopside + 1.5 orthoenstatite + β-quartz + H_2O. American Mineralogist, 76, 1931–1939.

Yang, H. and Evans, B.W. (1996) X-ray structural refinements of tremolite at 140 and 295K: Crystal chemistry and petrologic implications. American Mineralogist, 81, 1117–1125.

Yin, H.A. and Greenwood, H.J. (1983) Displacement of equilibria of OH-tremolite solid solution. I. Determination of the equilibrium *P-T* curve of OH-tremolite. EOS, 64, 347.

Manuscript received February 24, 1997
Manuscript accepted February 6, 1998
Paper handled by Robert W. Luth